Master Thesis | Climate Physics | August 2020

Deposition of Organic Matter on Alpine Snow

Grant Francis

Supervisor: Rupert Holzinger

2nd Supervisor/ Reviewer: Thomas Röckmann

Daily Supervisor: Dušan Materić

Universiteit Utrecht

IMAU Institute for Marine and Atmospheric research Utrecht

ZAMG Zentralanstalt für Meteorologie und Geodynamik

INTER ⇄ ACT

IONICON

Abstract

There is currently minimal research that investigates the deposition and re-volatilization of organic matter (OM) on snow. Understanding this balance for individual organic compounds has the potential to provide more additional valuable information about past and present atmosphere-biosphere interactions. OM captured in the blank canvas of snow can reflect corresponding signatures of atmospheric OM once their deposition and re-volatilization rates are known. Furthermore, understanding this link between organics in the atmosphere to those found in surface snow will allow for improved interpretations of OM that is eventually preserved in glacial ice. This research builds on a recent pilot study by Materić et al. (2019) which investigated the post-precipitation change of OM in surface snow near the Sonnblick Observatory in the Austrian Alps using thermal-desorption proton transfer reaction mass spectrometry (TD-PTR-MS). This research now widens this investigation with an array of surface snow samples taken every alternate day at the observatory and around the surrounding area. Each sample was analyzed using TD-PTR-MS with both filtered and unfiltered protocols to differentiate detected micro and nano scale particles. An assessment of the sample data shows a high correlation between the OM found at the observatory and surrounding sampling locations, as well as a positive detection of nanoplastics using a fingerprinting algorithm developed by Materić et al. (2020). PTR-MS measurements of atmospheric OM in conjunction with meteorological data also recorded at the observatory throughout the snow sampling period suggests a possible link between surface snow OM and a pollution event characterized by a shift in wind direction.

Keywords: TD-PTR-MS, organics, alpine snow, atmospheric composition, nanoplastics

Contents

Introduction

By piecing together glimpses of the Earth's past climate history using some of nature's oldest climate records, climatologists have been reshaping our perspective of the current climate crisis. Some of these natural records can be preserved in the form of tree rings and can go back several hundred years (Loader, 2019), while others can be preserved in ice and can go back over two million (Dahl-Jensen, 2018). Trapped dust and isotopic ratios preserved in ice cores provide unique proxies for past atmospheric composition and temperatures (Lambert, 2008; Fischer, 2007; Brook, 2007; Thompson, 1995), and knowing the relation between gasses and temperature can provide important feedback for tuning climate models. Other particles such as trace organic matter have the potential to provide even more detailed reconstructions of past atmospheric compositions. Before any of this organic matter (OM) can become frozen in ice however, it must first be deposited on the surface snow layer. The dynamics of said OM depositing on snow surfaces is not yet well studied, and therefore the relationship between OM in ice and in the atmosphere when the snow layer was formed cannot yet be accurately determined.

This research is part of an ongoing study to understand the deposition and re-volatilization of OM in surface snow. These measurements build on recent preliminary research by Materić et al. (2019) which was the first application of the new thermal-desorption proton transfer reaction mass spectrometry (TD-PTR-MS) technique used to investigate the post-precipitation change of OM in surface snow near the Sonnblick Observatory in the Austrian Alps. This prior research successfully quantified a variety of organics in surface snow samples and presented simple mass balance models to describe their dynamics. Building on these preceding findings, this research broadens this study by now including a full array of surface snow samples encompassing a larger area at and around the observatory to evaluate how well OM in snow samples collected at or near the observatory represent OM found around the surrounding mountain area. In addition, this research includes an unfiltered protocol alongside the previously used filtering method to detect any larger OM that may have been removed from during the filtering process. Cross examination of surface snow OM data with meteorological and atmospheric PTR-MS measurements recorded at the observatory during the sampling period provide

possible connections between anthropogenic signatures found in both snow and atmospheric measurements.

Environmental pollutants, such as micro and nanoplastics found in snow today also present clear records of anthropogenic activity. Although the majority of research for microplastics pollution is generally focused within marine environments, the recent ongoing discoveries of micro and nanoplastics pollution in remote areas such the French Pyrenees (Allen, 2019), Alps (Materić, 2020) and Arctic alike (Bergmann, 2019), present yet more evidence communicating the impact and extent of global plastics pollution. It is estimated that if current production and waste management trends continue, roughly 12,000 metric tons of plastic waste will be in landfills or the natural environment by the year 2050 (Geyer, 2017).

This research contributes to the investigation of plastics pollution in remote alpine environments by testing for both micro and nanoplastics in the snow samples collected during this campaign. The sensitivity and mass resolution of the TD-PTR-MS method in combination with the recent development of a micro and nanoplastics fingerprinting algorithm by Materić et al. (2020) has made it possible to identify and quantify a variety of different micro and nanoplastic polymers in snow samples with concentrations as low as the ng/mL level. This fingerprinting algorithm checks for specific common polymers including polyvinyl chloride (PVC), polyethylene terephthalate (PET), polypropylene (PP), polypropylene carbonate (PPC), polystyrene (PS), and polyethylene (PE). The largest groups in total non-fiber plastics production are PE (36%), PP (21%), and PVC (12%), followed by PET, polyurethanes (PURs), and PS (<10% each), while polyester, most of which is PET, accounts for 70% of all polyester, polyamide, and acrylic (PP&A) fiber production. Altogether, these seven groups account for 92% of all plastics ever made (Geyer, 2017).

Ultimately the long-term goal of this research is to connect biogenic/anthropogenic organic signatures seen in surface snow OM with atmospheric OM. Once this is possible, then it will become easier to decipher the originations of OM found in ice cores which will add valuable information that could better enable scientists to piece together the sophisticated history of our past climate. Long term sampling of surface snow will eventually be needed to provide more data to definitively connect snow organics with atmospheric anomalies (due to the complexities involving re-volatilization and photo

degradation etc.), however within the relatively short time period of this campaign, it is likely that an atmospheric pollution event may have already been recorded in the OM signatures measured in this set of surface snow samples.

1 Theory

1.1 PTR-MS

Developed over 20 years ago, proton transfer reaction mass spectrometry (PTR-MS) has played a major role in a variety of research fields including medical/biotechnology applications (Brunner, 2010; Moser, 2005; Hansel, 1995), food sciences (Fiches, 2014; Déléris, 2011) and atmospheric science; particularly in trace gas and volatile organic compound (VOC) measurements (as referenced throughout this thesis). PTR-MS has continuously proven its impressive superiority over gas chromatography (GC) and other traditional measurement techniques for on-line trace gas and VOC analysis because of its inherent high mass resolution and quick response time (Jordan, 2009). While some PTR-MS instruments utilize quadrupole filters for ion separation of product ions formed in the reaction drift tube, modern PTR-MS instruments profit from incorporating a time-of-flight mass spectrometer which enables the detection of VOCs at concentrations as low as a few pptv with a high mass resolution of 6000 m/Δm (Jordan, 2009).

The underlying reaction kinetics behind PTR-MS take advantage of the specific proton affinity of H_2O relative to the proton affinities of the components found in clean air and of most organics. H_2O has a proton affinity of 7.22 eV (Lias, 1988) which is just inside the lower scope of most organic molecules' proton affinities which range from 7 to 9 eV (Hansel, 1995). This makes the proton transfer reaction between H_3O^+ ions and organic molecules mostly exoergic, but with low enough exoergicity that there is minimal breakup of neutral products (Hansel, 1995). Organics entering through a sample gas inlet, and H_3O^+ ions emanating from a hollow cathode ion source are allow to collide in the PTR drift tube section (figure 1) and undergo the following reaction:

$$H_3O^+ + M_iH_j \rightarrow M_iH_{j+1}^+ + H_2O \qquad (1)$$

where M is a combination of C, O, N and S atoms. The reaction rate coefficients of these processes are fast, with coefficients close to the Langevin rate coefficient: $k_0 \approx 10^{-9}$ cm^3 s^{-1} (Hansel, 1995).

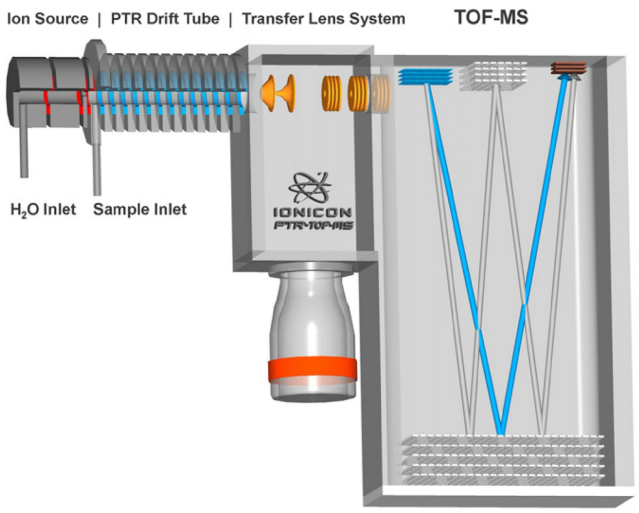

Figure 1. Diagram of the PTR-ToF-MS instrument illustrating the hollow cathode ion source, drift tube collision section, transfer lens system, and time-of-flight mass spectrometer (with V- and W-operational modes outlined in blue and grey respectively) (Jordan, 2009).

H_3O^+ ions are ideal proton donors when probing for trace organics in air because H_3O^+ does not react with any of the common components in air as their proton affinities fall below that of H_2O (Hansel, 1995), thus they do not contribute to any significant loss of H_3O^+. There can be however some loss resulting from association reactions primarily with H_2O forming $H_3O^+ \bullet H_2O$ through the following ternary reaction:

$$H_3O^+ + H_2O + M \rightarrow H_3O^+ \bullet H_2O + M \quad (2)$$

where M is any neutral partner which collides with and stabilizes the excited $(H_3O^+ \bullet H_2O)^*$ complex formed from H_2O and H_3O^+ binary collisions. The reaction rate of this loss was found to have a strong negative dependence (Bierbaum, 1976) with E/N (electric field strength per buffer gas number density within the PTR drift section), which enables a significant reduction in H_3O^+ loss with sufficiently high E/N (Hansel, 1995).

From here the ions are accelerated into the TOF section using the transfer lens system at a typical repetition rate of up to approximately 80 kHz (Jordan, 2009). During each pulse, ion flight times are proportional to each ion's mass to charge ratio thus giving a full mass spectrum (figure 2) for each

interval which is recorded via high speed data acquisition (Jordan, 2009) and stored on a desktop computer.

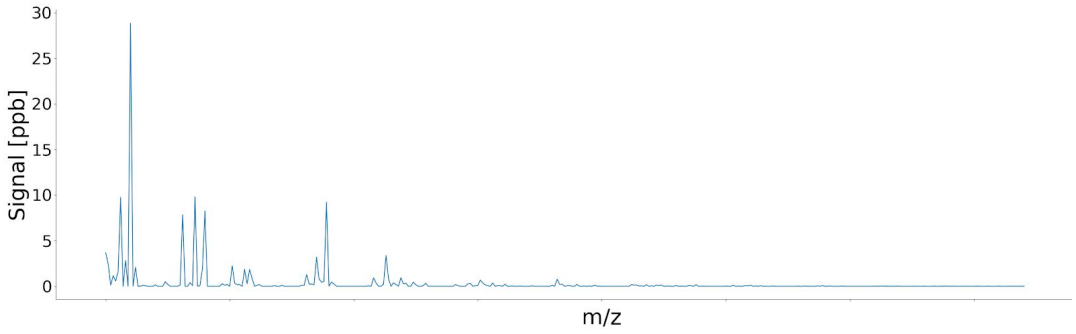

Figure 2. Example of a typical mass spectrum signal from a PTR-MS measurement depicting concentrations of detected ions ranging in mass from 20 m/z to 500 m/z.

1.2 TD-PTR-MS

Thermal desorption coupled with proton reaction mass spectrometry (TD-PTR-MS) is an innovative new technique recently developed by Materić et al. (2017) which now allows for the measurement of OM in liquid samples using PTR-MS. The technique (as described in section 2.2.3) involves first the careful removal of water from the sample using a clean, low-pressure evaporation/sublimation (LPE) system (figure 3a) which was adapted to limit the loss of the organic (semi-volatile) fraction of the sample and limit any contamination from laboratory air (Materić, 2017). Once dehydrated, the samples are slowly re-pressurized again to atmospheric pressure using nitrogen, and then sealed with clean Teflon caps until analysis using the TD-PTR-MS system (figure 3b). Samples loaded into the TD oven are heated using an arduino controlled temperature profile starting at 35 °C and slowly ramping up to 350 °C. OM left behind in the sample after LPE that is thermally desorbed during this heating process is then transferred to and measured by the PTR-MS system using a background flow of 50 mL min^{-1} of clean air. Figure 4 shows a typical individual ion signal measured by PTR-MS during the thermal desorption cycle for six sequential sample runs.

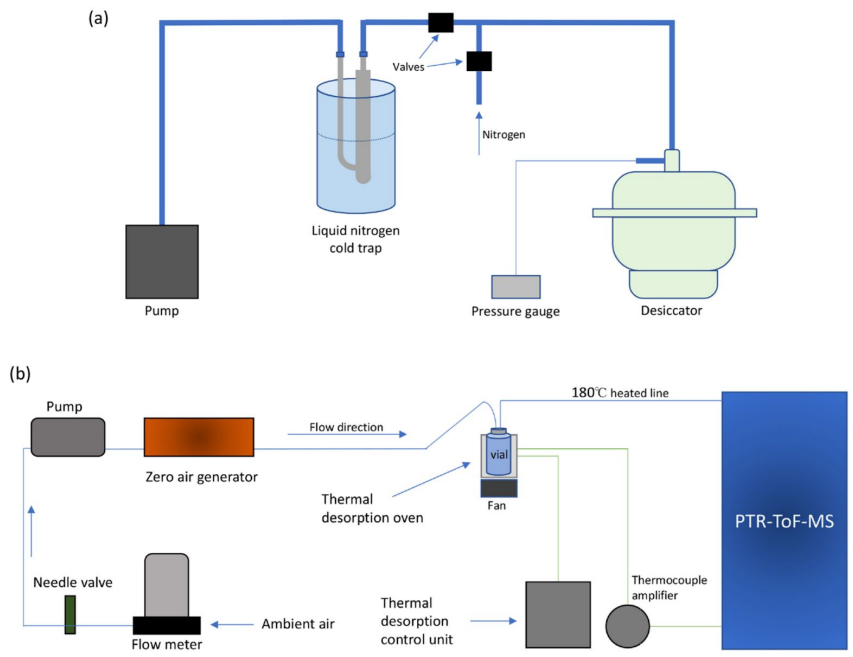

Figure 3. (**a**) Schematic of the low-pressure evaporation/sublimation (LPE) system. (**b**) Schematic of Thermal Desorption (TD) system coupled with the PTR-ToF-MS instrument (Materić, 2017).

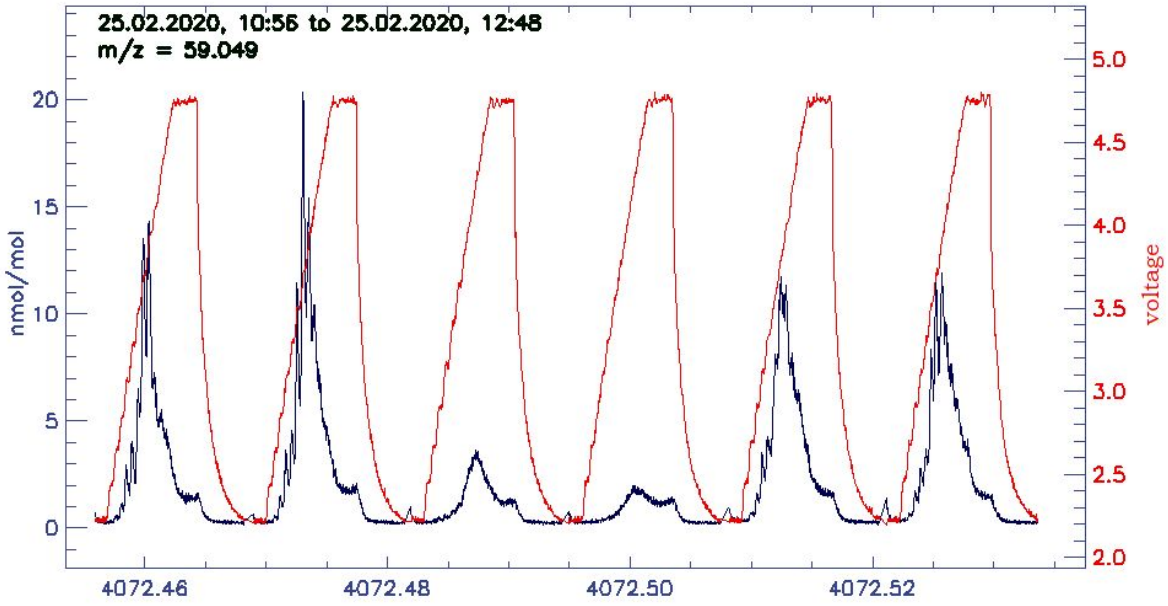

Figure 4. Individual ion signal for 59.049 m/z (navy) and analog voltage for TD oven (red) recorded by PTR-MS during the thermal desorption cycle for six sequential sample runs.

2 Methods

2.1 Identifying Air Pollution

The atmospheric pollution event referred to in this research is characterized by pronounced anomalies within CO_2, CO, benzene and toluene measurements recorded at Sonnblick between December 12th and 14th which coincide with substantial changes in wind trajectory during this period. CO_2 and CO data were provided by the Austrian Federal Environment Agency, while three key OM signals that are associated with anthropogenic emissions (acetonitrile, benzene and toluene) detected by PTR-MS during the period were analyzed to discern the nature of the emission sources (e.g. industry, vehicle emissions, biomass burning etc.). Both vehicle emissions and biomass burning are known sources of CO_2 and CO (Jabali, 2012; National Research Council, 2002; Andreae, 1988; Crutzen, 1979) as well as benzene and toluene (Tawfiq, 2015; Baimatova, 2015; Adamovic, 2012), however acetonitrile has been shown to be a marker of biomass burning, even in areas with high levels of vehicle emissions (Holzinger, 2001, 1999).

The patterns observed in these OM signals for acetonitrile, benzene and toluene were compared with the CO_2 and CO measurements to determine their likely association with the pollution anomaly thus differentiating a source signature. The timing and proportion of this pollution event also provides a possible explanation for the trend seen in this campaign's surface snow sample measurements with total OM (<0.2μm) concentrations over the span of the sampling period having the largest concentration at all sites on the first day, and then regularly decreasing over the following days. This is consistent with an impulse OM deposition that would be expected following a pollution event.

2.2 Surface Snow Array

2.2.1 Location

The Sonnblick Observatory location presents an ideal candidate for collecting surface snow samples for OM research as this remote mountaintop is distant from any dense urban areas with high levels of OM pollution. It however remains necessary to assess if snow samples collected at the Observatory are indeed representative of the snow around the surrounding area, and to identify (if any) local contaminants originating from the Observatory.

The Sonnblick Observatory research station is situated at the summit of Mt. Hoher Sonnblick in Austria at an elevation of 3106m. Data gathered at the station since its construction in 1886 show an average temperature at the site of about 1.1 °C in summer and −12.2 °C in winter (data provided courtesy of Zentralanstalt für Meteorologie und Geodynamik (ZAMG)). The array of snow samples consisted of sites located around the plateau that is above the Kleinfleißkees glacier between Mt. Hoher Sonnblick, Goldbergspitze and the Observatory, as well as multiple sites at the Observatory itself (figure 5). Each of the sampling sites on the plateau were given a number from 1 to 6, while the samples collected at the observatory rooftop measuring deck and northside measuring deck were labeled accordingly. Duplicate samples were taken at the observatory rooftop for the purpose of assessing any inconsistencies at this site for future long-term sampling, and for gauging overall the variability of the sampling method in general. The sample taken on the northside measuring deck at the observatory was the closest to the inlet for the PTR-MS measurements of atmospheric OM which was actively recording during the sampling period. Samples labeled 1-6 taken throughout the surrounding area encompass sites up to 500 m away from the Observatory, ultimately delineating a large triangle with the Observatory bisecting the northernmost side. Sites 1-3 were chosen as the farthest reaching corners of the array with noticeably nearby rock outcroppings. Sites 4-6 partitioned the center of the array and are uniformly distributed about the col between Mt. Hoher and Goldbergspitze.

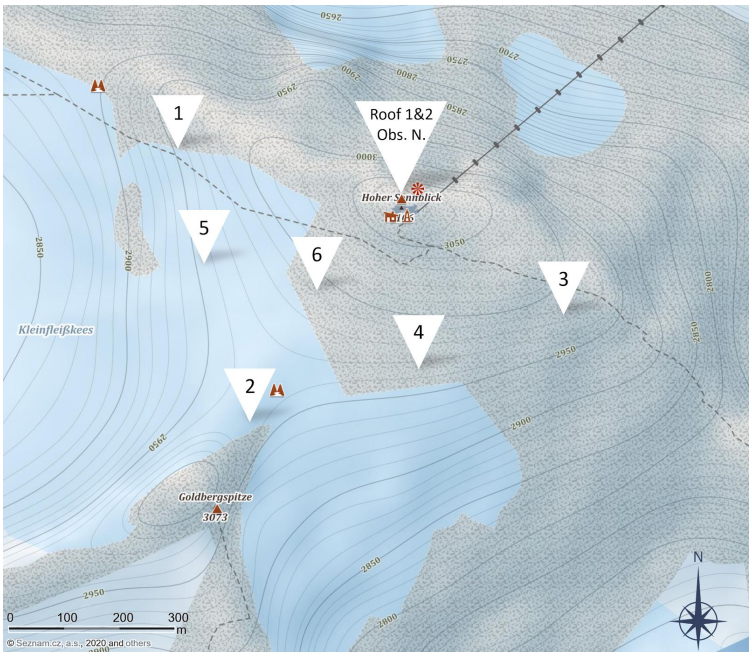

Figure 5. Map of the array of surface snow sampling sites depicting their relative positions to each other and among the local topography and other landmarks (Kleinfleißkees glacier, Goldbergspitze etc). Observatory sites are abbreviated by Roof 1, Roof 2, and Obs. N. indicating the duplicates taken at the rooftop measurement deck and the northside measurement deck respectively. Field locations are numbered 1-6, with 1-3 being the far corners of the array and are near noticeably protruding rock outcroppings, while 4-6 are evenly distributed along the col between Goldbergspitze and Mt. Hoher Sonnblick.

2.2.2 Sampling

Snow samples were collected on the 14th, 16th and 18th of December 2019. For each of the three days, a full array of samples was collected for a total of 26 samples. (Due to unfortunate circumstances, the sample taken at site 2 on the 16th of December was lost on the mountain and therefore could not be included in this research). Sampling occurred in the late morning and took less than two hours to obtain the complete array. Conditions were typically consistent during the sampling period with generally low visibility and high winds. For the duration of the sampling period, the average wind speed was 14 m/s, with an average 2 m temperature of -8.8 °C at an average pressure of 685.7 hPa. Ten-minute averages of 2 m temperature, humidity, wind direction/speed are shown in figure 6.

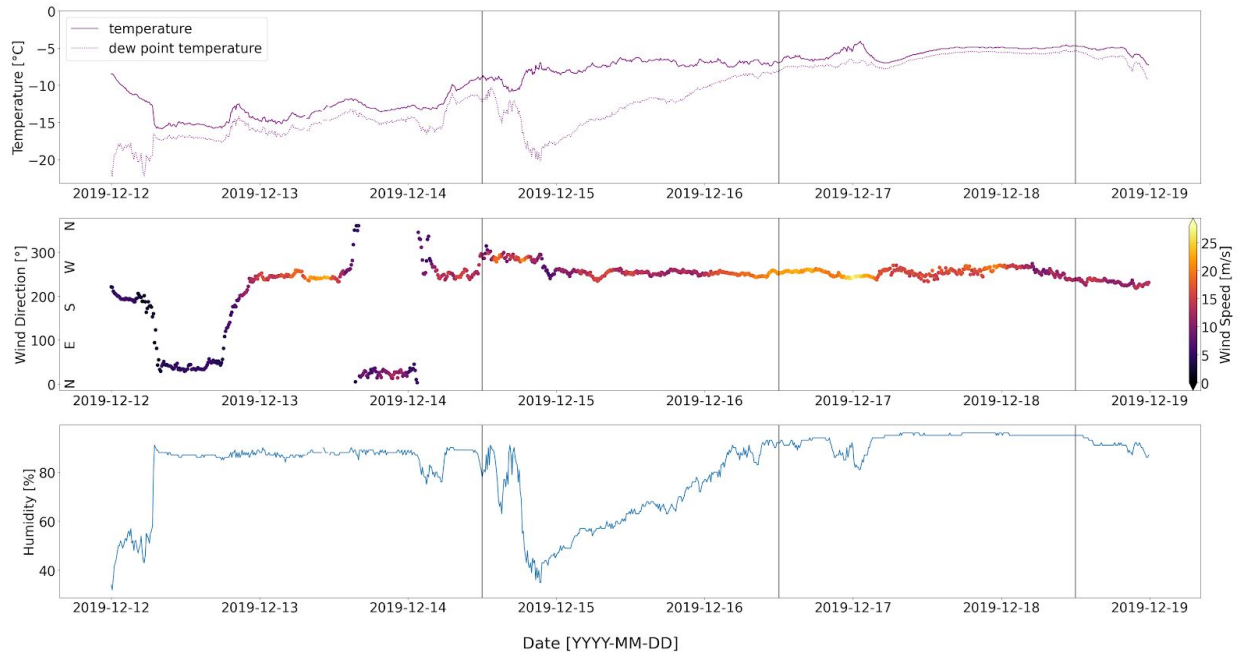

Figure 6. 10-minute averaged temperature, dew point temperature, wind speed/direction and humidity measurements recorded at Sonnblick during the snow sampling campaign. Vertical black lines indicate time when surface snow sample arrays were collected. Data provided courtesy of Zentralanstalt für Meteorologie und Geodynamik (ZAMG).

To obtain a snow sample, a clean 60 mL glass vial was placed open-end down on the snow surface and gently pressed into the snow until the bottom of the vial was level with the snow surface. Upon careful recovery of the vial, the snow clinging to the inside would yield an extracted cylindrical sample of surface snow (<3 cm in depth) and with consistent diameter/surface area throughout all samples. The sample was then sealed with the vial's PTFE cap and frozen at -20 °C until the end of the campaign when all were returned to the analysis lab and stored at -20 °C until analysis. Field blanks using distilled water exposed to the same sampling conditions were also collected and analyzed equally to the surface snow samples for the purpose of ruling out possible impurities that may have been introduced from any mountaineering equipment used during sampling excursions.

2.2.3 Analysis

The analysis procedure for this study was nearly identical to the procedure described in (Materić, 2019). After slowing melting the snow sample by equilibrating to room temperature, a set of 1 mL unfiltered triplicates and 1 mL filtered triplicates were made from each sample. Unfiltered replicates were first homogenized by inverting the sample twice and then were pipetted directly into clean 10 mL glass vials used in the low-pressure evaporation–sublimation system and analyzed by TD-PTR-MS (PTR-TOF 8000, IONICON Analytik) using the method described by (Materić, 2017). Filtered replicates were made similar to their unfiltered counterparts, but by first filtering an aliquot of the homogenized sample through a PTFE 0.2 μm filter, and then were pipetted and analyzed identically as the unfiltered replicates. Corresponding blanks (for both the unfiltered and filtered replicates) using Milli-Q ultrapure water were prepared using identical procedures. Sample replicates and blanks were measured in random order with PTR settings of: 2.8 mbar, 120 °C drift tube pressure and temperature, and *E/N* of ~107 Td. The thermal desorption temperature profile used initiated with a 1.5 min incubation period at 35 °C and increased to 350 °C at a rate of 40 °C min^{-1}, remained at 350 °C for 5 min, and then cooled again to 35 °C for a total run time of roughly 20 min. In total, six consecutive days were needed to measure all sample and blank replicates. All data was stored on the lab desktop computer.

Data analysis was primarily done using the custom software PTRwid developed by Holzinger (2015) in conjunction with scripts written in python for further statistical evaluation (all python scripts were written myself for the purpose of data analysis for this project and can be viewed at: https://github.com/G-Francis/Dep_of_OM_Alps_MSc_Thesis.git). Within PTRwid, the PTR-MS measurement data was extracted using the Average and Merge Data tool (Holzinger, 2015). Identified peaks within the mass spectra of each replicate were quantified by integrating for 10 min from the moment the TD profile reached 50 °C. In this research, OM is defined by ion signals in the mass spectra corresponding only to organic compounds. The limit of detection (LoD) was defined by 3σ of the ion signals in the ultrapure blanks, thus any quantified signal detected in the respective replicates falling below this threshold was not considered statistically significant and omitted from results. Both filtered and unfiltered blanks were also compared against system blanks to check for any

contamination that may have been introduced with the pipetting and filtering procedures. Comparatively low levels of impurities were found with only 9.5 ng/mL and 6.8 ng/mL for the unfiltered and filtered lab blanks respectively, which are consistent with the level of impurities found in the field blanks in (Materić, 2019) using the same ultrapure water. Most notably 63.023 m/z was found to contribute up to 60% in some of the unfiltered blanks while 121.065 m/z was found to contribute up to 50% on average to the impurities in the filtered blanks. These impurities were ruled out in sample analysis by method of subtraction and LoD filtering (Materić et al., 2017). Resulting levels of detected ions were expressed in ng/mL. In order to quantitatively compare the similarity of the ions detected between two sampling sites, R^2 correlations were calculated from each site's resulting mass spectra of organic ions after blank subtraction and LoD filtering. Sites with R^2 >0.7 are considered to contain significantly similar organic ion fingerprints.

2.3 Micro & Nanoplastics Detection

The data used for this analysis is the same extracted mass spectra data obtained from each of the sampling sites (again with a 3σ LoD threshold and blank subtraction as described in section 2.2.3 of this research). The fingerprinting algorithm used takes into account only ions >100 m/z in the mass spectra as masses below this are dominated by thermal dissociation products of nonvolatile high-molecular-weight organic compounds (Materić, 2020, 2019). By first selecting the highest ion signals in the mass spectra, the algorithm normalizes the 40 largest peaks to the largest peak detected, and then computes the absolute difference between the normalized concentration of the sample and the normalized concentration of library ions from a standard, with the difference weighted by the library ion's relative concentration (Materić, 2020). Thus, the algorithm's match score (mass spectra similarity) is calculated by , where is the match score percentage and is the absolute difference (Materić, 2020). Only samples with a match score above a mean and 2σ of the score generated on 1000 random mass spectra (z-score 2, p-value <0.02275 – one tail distribution) (Materić, 2020) are included for this study. Matches within data obtained through the unfiltered analysis protocol are attributed from both nanoplastics and microplastics (within the μm regime and smaller than mm regime, as no

plastic particles were visually observed in any of the samples), while matches within filtered data indicate only nanoplastics.

3 Results

3.1 Connections with Air Pollution

3.1.1 Atmospheric Observations

Meteorological data collected at the Observatory spanning the days leading up to and during the snow sampling period show significant deviations in wind trajectory for several hours on December 12th, and the night of 13th – 14th. These fluctuations show a sudden shift to steady northerly- northeasterly (~30° NNE) winds, while the predominant wind direction for this period is consistent westerly/ southwesterly (~250° WSW) (figure 6, 7).

During this time, gas measurements at the Observatory show elevated levels of CO_2 and CO with an increase of 2 ppm and 20 ppb respectively in the following hours after the first shift in wind heading. There is a brief period of decline during this peak (indicated by the black arrows in figure 7) in which both signals begin to decrease on the early morning of Dec. 13th which is consistent with the wind momentarily returning to its original WSW heading before once again turning NNE in the evening of Dec. 13th. At this point, both CO_2 and CO levels begin to rise again until reaching roughly a maximum that late evening/night, and then begin to fall to their background levels once again by the afternoon the following day. This is equally coherent with the wind returning to and remaining at its original heading the night of the 13th – 14th.

PTR-MS measurements of toluene and benzene both show an unmistakable resemblance (R^2 >0.7) to the same rising and falling pattern that characterizes this anomaly with both rising roughly a maximum of 40 ppt above their background levels. Although the signal for acetonitrile does indeed display a subtle adjustment during this period, there does not appear to be any obvious similarities (R^2 <0.4) to the distinguishable pattern of the pollution event previously described.

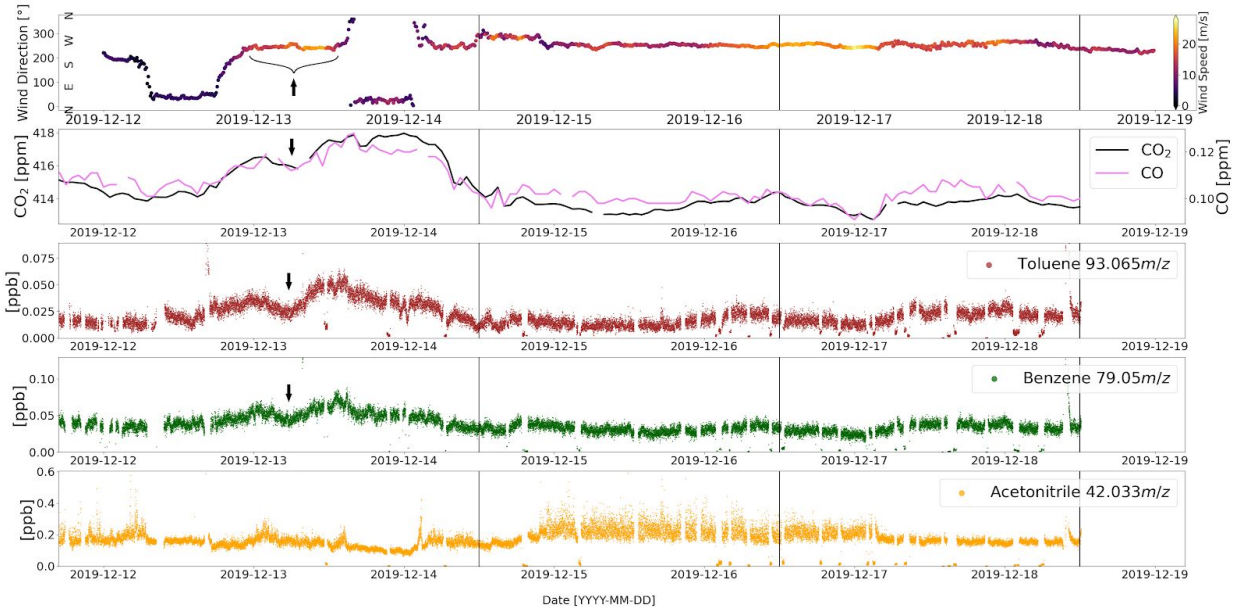

Figure 7. Measurements for wind direction/speed, CO_2, CO, toluene (93.065 m/z), benzene (79.05 m/z), and acetonitrile (42.033 m/z) recorded at Sonnblick during the course of the pollution event and over the duration of the surface snow sampling campaign. The relative dip in concentration experienced by CO_2, CO, toluene and benzene corresponding with the temporary fluctuation in wind direction are indicated by the black arrows. Vertical black lines indicate time when surface snow sample arrays were collected. CO_2 and CO data were provided courtesy of the Austrian Federal Environment Agency.

Gas Signal and PTR-MS Signal Correlations (R^2)

m/z	formula	name	CO_2	CO
93.065	$C_7H_8H^+$	toluene	0.70	0.71
79.05	$C_6H_6H^+$	benzene	0.70	0.74
42.033	$C_2H_3NH^+$	acetonitrile	0.35	0.30

Table 1. Detected peak mass [m/z] with attributed chemical formula/name and corresponding correlation with both CO_2 and CO signals during the pollution event.

3.1.2 Surface Snow Observations

The surface snow samples collected during this campaign not only reflect consistencies in OM measured at the Observatory and the other surrounding sites (section 3.2), but also the total concentration of OM (<0.2 μm) measured at all of the sites also appears systematically highest in the samples obtained on Dec. 14th (with the exception of the Observatory sites on Dec. 18th as discussed in 4.2), with an overall average site total OM concentration of >70 ng/mL. Over the ensuing days, the average concentration of OM at all sites appears to decrease linearly at roughly 10 ng/mL day^{-1} when neglecting possible Observatory contaminants on Dec. 18th (figure 8b). The most notable ion signal detected at all sites (using both the unfiltered and filtering procedures) that also imitates this trend is the ion detected at mass 101.092 m/z, with concentrations also significantly elevated at all array sites on the first day (figure 9a).

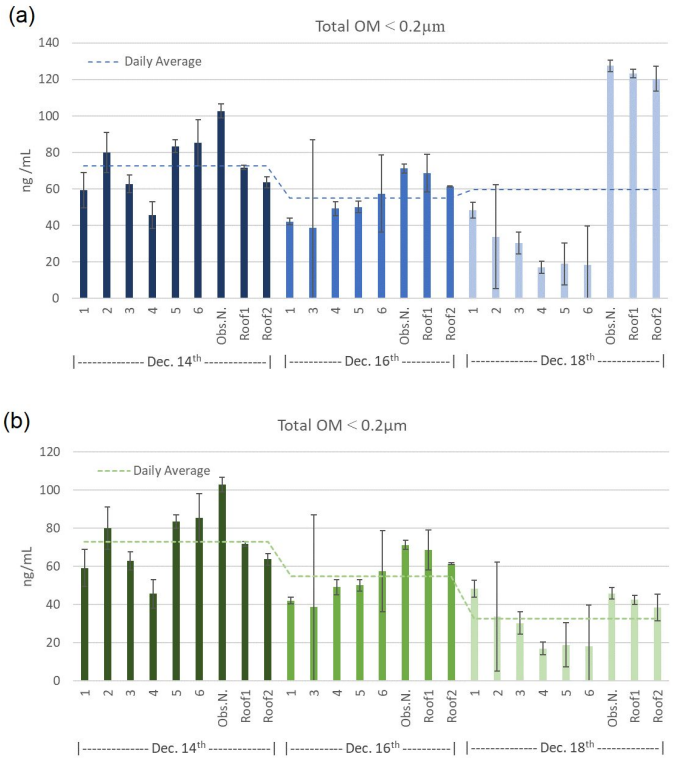

Figure 8. (**a**) Total filtered OM (<0.2 μm) in ng/mL from all array sites on all three days of the sampling campaign with daily average concentration notated by the dotted line. Error bars shown here are the standard deviation of the total OM detected in the three replicates measured for each sample. The Observatory sites on December 18th show notably higher total concentrations with main contributions from 45.033 m/z (13%), 55.041 m/z (30%), 61.028 m/z (12%) and 63.023 m/z (13%). It is likely these may be contributed to local contaminants from the Observatory as these are not ever seen in any other field sites at these exceeding amounts. (**b**) Neglecting these contaminants, the overall average site concentration reveals a constant decrease of ~10 ng/mL day^{-1}.

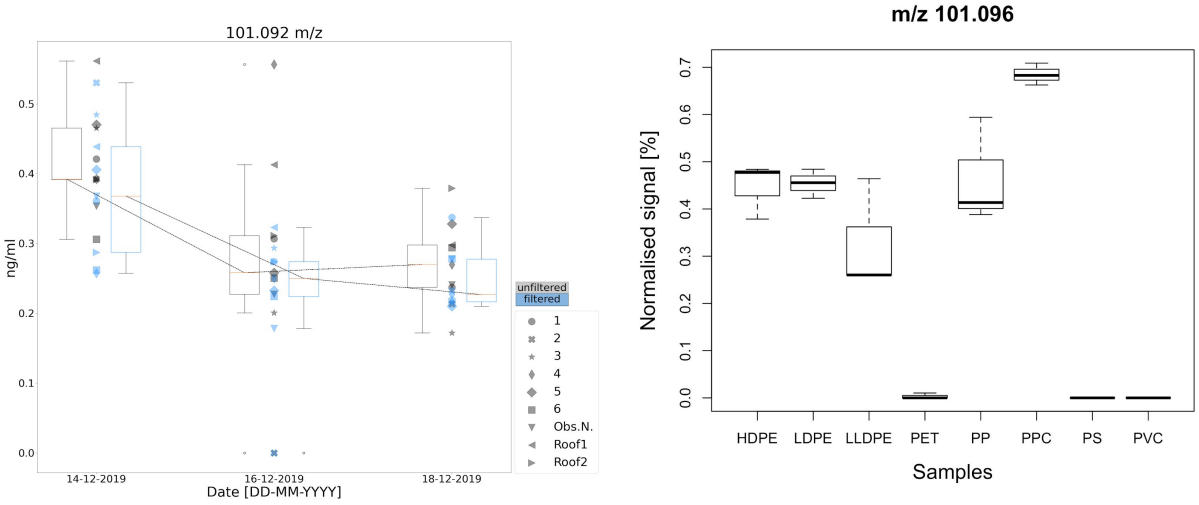

Figure 9. (**a**) Surface snow concentration of ion 101.092 m/z in all array samples on Dec. 14th, 16th, and 18th with results from the unfiltered analysis in grey and filtered analysis in blue. (**b**) Ion signal 101.092 m/z previously detected similarly at mass 101.096 m/z and its corresponding normalized concentrations found in PE and PP fingerprinting (Materić, 2020).

3.2 Sample Site Correlations

Mass spectra correlation analysis of all samples collected at both the beginning and end of the campaign (December, 14th and 18th) overall show a relatively high agreement between OM found at the Observatory rooftop measurement deck and all other sites in the array. The resulting R^2 from each of the mass spectra comparisons with the rooftop site are listed in table 2. All comparisons between Observatory samples (duplicates from rooftop measuring deck and northside measuring deck) have an exceptionally high correlation (R^2 >0.7) with each other. The comparisons between the surrounding field sites with the rooftop site range from as low as 0.18 to as high as 0.97, with the majority of sites exhibiting significant resemblance to each other (R^2 >0.7) across both filtered and unfiltered data for both days. One important distinction that sets apart some of the field sites from each other is that samples collected from the plateau all consistently have high correlations (R^2 >0.7) with the rooftop, while the more remote corner sites often fall short of this.

Sampling Sites Mass Spectra Correlation (R^2)				
	Dec. 14th		Dec. 18th	
Site Label	(filtered)	(unfiltered)	(filtered)	(unfiltered)
1	0.88	0.74	0.45	0.18
2	0.13	0.65	0.44	0.71
3	0.25	0.75	0.39	0.45
4	0.85	0.96	0.97	0.73
5	0.90	0.86	0.81	0.94
6	0.74	0.83	0.72	0.95
Obs. N.	0.94	0.72	0.96	0.93
Roof 2	0.85	0.94	0.83	0.84
Roof 1	1.00	1.00	1.00	1.00

Table 2. Mass spectra correlations (from both filtered and unfiltered data) between all sampling sites compared with the rooftop measurements deck. Because the majority of the sites exhibit R^2 >0.7, the local variability is generally less than 30%.

3.3 Micro & Nanoplastics Matches

Data from the unfiltered analysis reveals positive fingerprinting matches from all array sites on all three days for several micro and nanoplastic polymers. Figure 10 presents the resulting matches and their concentrations as ng mL^{-1} from each of the sampling sites throughout the campaign. Concentrations from each match from this test are assumed to have contributions from both nanoplastics and microplastics (within the μm regime and smaller than mm regime, as no plastic particles were visually observed in any of the samples). Because fingerprinting for polypropylene (PP) and polypropylene carbonate (PPC) have almost indistinguishable signatures, the results presented here regard them conjointly.

Data from the filtered analysis however also exhibited two positive matches with PP and PE, with these appearing at site 5 and all three Observatory sites on the first day of the campaign (figure 11). Concentrations from positive matches within filtered snow data remove any contribution from microplastics and are therefore the result of nanoplastics (<0.2 μm) only. The concentrations shown here for PE (~6 ng/mL) and PP (~15 ng/mL) resemble less than 20% of total filtered OM seen in

figure 8a, however when taking into consideration the 5% dissolved organic matter (DOM) fraction seen by TD-PTR-MS (Peacock, 2018), these concentrations account for roughly 1% of the DOM. Both field blanks and lab blanks used for each analysis (filtered and unfiltered) were also checked with the fingerprinting algorithm and showed no indication of any positive matches.

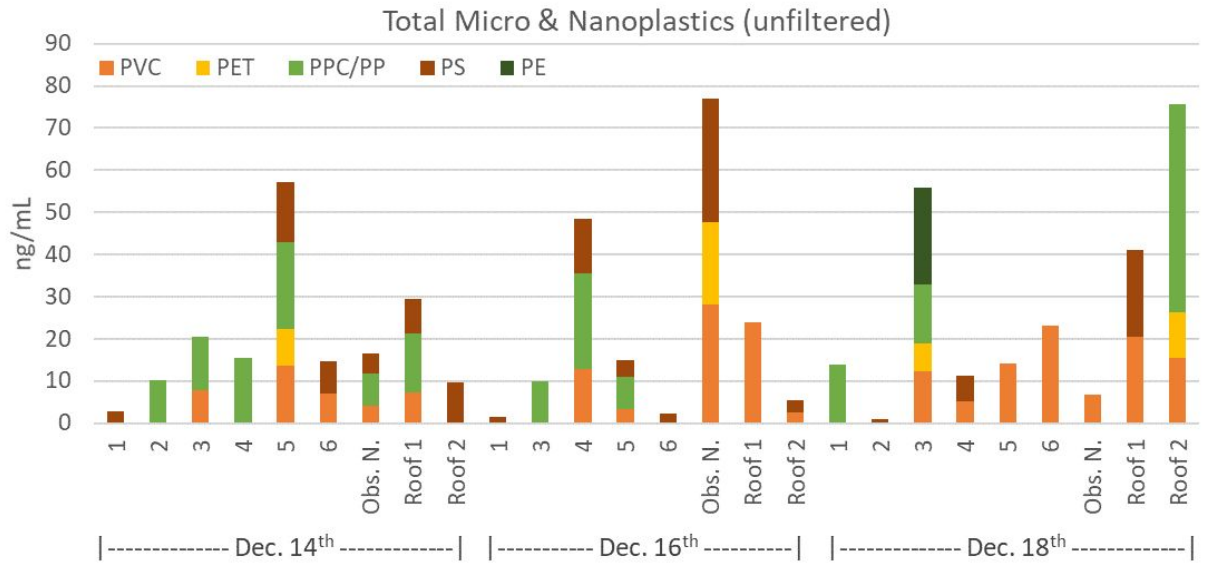

Figure 10. Resulting concentrations of plastics exhibiting positive matches within the unfiltered surface snow data at each of the sampling sites on all three days of this campaign.

Figure 11. Positive matches for PE and PP nanoplastics within the filtered snow data on the first day of this campaign. Error bars shown here are the standard deviation of the total OM detected in the three replicates measured for each sample.

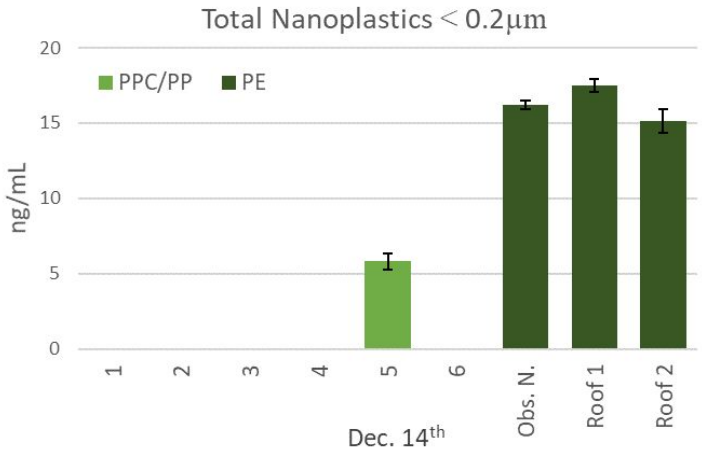

4 Discussion and Outlook

4.1 Pollution: From Air to Snow

With changes in wind direction, different air masses that are brought to Mt. Hoher Sonnblick carry with them different atmospheric composition and different OM which hold certain clues about the environment from which they came. These fluctuations are detected with the sensitive instruments at the Sonnblick Observatory and measurements with correlated trends suggest a distinct affiliation with each other and the pollution event, which ultimately provides a unique signature of the environment from where they originated. While CO_2 and CO emissions alone can be indicators of anthropogenic activity, clear relationships shown here with toluene and benzene reveal even stronger evidence for anthropogenic origin. The lacking relationship with acetonitrile measurements at this time however rules out biomass burning (e.g. forest fire, wood stoves etc.) as a source therefore narrowing the likely explanation for the pollution source to be vehicle emissions. This suggests that the air mass responsible for bringing the pollution emissions must have transported contaminants and other OM from an urbanized area that would not have normally reached the mountain. Although the signatures of these OM contaminants measured in the atmosphere may not be identical to the signatures measured in deposited surface snow OM (due to thermal disassociate products in TD-PTR-MS), there is still a record of these OM contaminants in snow nonetheless. This unique signature could potentially reside among other ions within the mass spectra of the snow samples. One such indication of this link between the atmospheric OM from this pollution event and the OM detected in the snow samples in this campaign is the substantially higher concentration of filtered OM (<0.2 μm) seen in the samples collected on the first sampling day, and the total concentration decreasing in all sites over the following days. This is possibly explained by a large amount of OM deposition during the pollution event just prior to the first sampling day.

Individual ions detected at each of these sampling sites that also follow this same pattern are likely associated with this event and could therefore provide a unique signature in TD-PTR-MS measurements of snow OM that are complementary to PTR-MS measurements of atmospheric OM.

Most notably it was found that the signal for 101.096 m/z (detected in all sites) exemplified this trend very closely, with all sites showing significantly higher levels on the first day (figure 9a). This ion is particularly interesting because it has already appeared in previous research as a significant tracer ion for PE and PP fingerprinting (Materić, 2020) (figure 9b), which is also consistent with the nanoplastics detected on the first day of this campaign (figure 11). This association with nanoplastics further supports the possibility that the higher concentration of surface snow OM on Dec. 14th is a direct consequence of contaminants from urban air pollution depositing on the snow. With more research and more surface snow measurements spanning a longer time period, it will be possible to capture additional vestiges from future pollution events and will enable the identification of more anthropogenic OM signatures in TD-PTR-MS research of surface snow OM.

4.2 Sampling from the Observatory

The strong coefficient of determination between two mass spectra indicates a high percentage of similar OM concentrations present in both samples. Correlations between two samples that are expected to contain similar OM (e.g. rooftop duplicates) also gives perspective for natural variability. For instance, the duplicate rooftop samples which were collected less than one meter apart from each other and nearly at the same time, one might expect to see virtually the same signature in both. This is however extremely unlikely given the nature of a mass spectra representing concentrations of over 300 different low-molecular-weight ions within a sample, and for this reason R^2 >0.7 can be interpreted as exceptionally high similarities between both samples.

Taking this significance level into account, the most notable result from this mass spectra correlation study is the high correlation between the rooftop and the field sites with the majority exhibiting R^2 >0.7. There is also a notable consistency among the more remote field sites near the rocky areas (sites 1-3) only occasionally showing resemblance, while the more homogeneous snowfield area (sites 4-6) invariably exhibiting a strong resemblance with the rooftop. This is not necessarily surprising because it suggests the possibility of these more remote sampling areas containing OM originating locally at these rocky regions that are not present at the observatory.

One important goal of this study is to determine whether or not samples taken at the Observatory would contain any local contamination, and to also rule out the possibility that field sites may only show a high resemblance to the rooftop because they too have trace contamination from the Observatory. This is exceedingly unlikely because the measured wind direction during the sampling campaign persistently places the field sites upwind from the Observatory. Also, because the four ions 45.033 m/z, 55.041 m/z, 61.028 m/z and 63.023 m/z detected in exceeding amounts at the Observatory sites on the December 18th (figure 8a) were not measured in high levels in any of the field sites, which supports the possibility that these are due to local contamination and should therefore be acknowledged in future samples collected from the Observatory. Even despite these contaminants, there still remains a strong correlation between the field sites and the Observatory sites, so it is unlikely that the samples collected at the observatory contain significant amounts of other local contamination, and instead accurately represent the majority of OM found throughout the surrounding area. This conclusion is majorly important for future snow sampling research conducted at the Observatory.

4.3 Plastics Pollution

The results presented in section 3.3 support the growing amount of evidence for microplastics pollution in our environment. When comparing the results from the unfiltered analysis data (both micro and nanoplastics) with the results from the filtered analysis data (only nanoplastics), it is evident that the majority of the plastic pollution found in these surface snow samples is due to plastics particles >0.2 μm but smaller than what can be visually observed. When considering the consistent amount of fresh snow that fell during the campaign, this result is consistent with previous findings that showed higher levels of nanoplastics are delivered to the snow surface by dry deposition during precipitation-free periods (Materić, 2020). This is also consistent with the findings of Brahney et al. (2020) that also states that plastics deposited under dry conditions were smaller in size, and the rates of deposition were related to indices that suggest longer-range or global transport. Nonetheless, it is possibly not by coincidence that the trace amounts of nanoplastics detected were found on the first of the three sampling days (Dec. 14th), as this could be a consequence of the pollution event that occurred the previous day (discussed in section 4.1).

One important note is the clear disagreement between the micro/nanoplastics result and the nanoplastics result is the detection of PE within the filtered snow data (nanoplastics), but not within the unfiltered snow data (micro and nanoplastics). From these results it appears as though PE was detected in higher loads when filtering than when not filtering the sample. Although puzzling at first glance, this discrepancy may be explainable by two likely occurrences. One likely cause is that the resulting mass spectra used in the fingerprinting of micro and nanoplastics could be dominated by signatures from relatively larger concentrations of OM due to the nature of the unfiltered analysis not removing larger particles, and therefore the unique PE signature could be masked by signatures from substantially higher concentrations of OM present in the data, thus reducing the algorithm match score (Materić, 2020). Another possible explanation that has not yet been ruled out is the prospect of a particular clumping behavior previously seen when preparing plastic standards for TD-PTR-MS nanoplastics fingerprinting research, which is thought to be the consequence of static charge. When preparing plastics standards, small plastic particles were observed to cling to the inside walls of glass vials, as well as form clumps by sticking to each other. This being the case, a systematic difference between the unfiltered and filtered analysis procedures could explain the discrepancy in detection. It is possible that if the nanoplastics particles are indeed statically charged, then they not only experience clumping, but also have the potential to stick to the inside of the glass vials used. If this is true, then it is likely the 1mL pipetted loads used in the unfiltered procedure are not sufficiently large enough, and can effectively miss these charged clumps. The larger aliquots pulled from the sample in the filtering procedure have a higher chance of capturing these clumps, and when they are forced through the PTFE 0.2 μm filter, these clumps break apart and re-homogenize within the sample which would allow for the subsequent 1 mL pipetted loads to capture a more accurate concentration of these particles. Because both of these scenarios are still hypothetical, more research is needed to better understand the behavior of these particles and interactions with the lab equipment used to further improve the sensitivity and limit of detection of this method.

Conclusion

This research demonstrates once again the impressive sensitivity of TD-PTR-MS for the detection and identification of OM in snow. Assessment of OM in surface snow samples from this campaign using this technique has shown that the snow collected at the Sonnblick Observatory accurately resembles the OM found elsewhere on the mountain, and therefore presents an ideal location for future snow sampling research. Together with a multitude of meteorological data, CO_2, CO and atmospheric PTR-MS OM measurements, this research also illustrates a preliminary example of determining specific TD-PTR-MS ion signatures from in surface snow for atmospheric OM anomalies. In this case, the ion detected at mass 101.092 m/z was identified as a likely candidate to be an indicator of anthropogenic contaminants deposited onto the snow because of the ion's association with nanoplastics fingerprinting, and also because of its relative concentration following an observed declining trend which is to be expected succeeding a previously identified pollution event. Algorithmic nanoplastics fingerprinting of each sample in this survey has also revealed a positive detection of several plastic polymers at both the micro and nano scales which contributes to the increasing amount of evidence exposing the true extent of environmental plastic pollution in remote areas like the Alps. With the promising potential of TD-PTR-MS analysis, in the near future it may be possible to solve the enigma of deposition and re-volatilization of OM on surface snow, and to eventually establish the connection between OM signatures trapped in ice and atmospheric conditions of past climate.

Acknowledgments

I would like to personally thank my supervisors for their support and feedback during the initial thesis review, with special thanks to Dr. Rupert Holzinger and Dr. Dušan Materić for their patience, attention to detail and dedication to the research. Your wealth of knowledge has been invaluable throughout the entirety of my thesis research process.

I also would like to thank the supportive lab group and technicians at IMAU, ZAMG, the Austrian Federal Environment Agency, and all those working at Hoher Sonnblick for making research like this possible. Dr. Elke Ludewig of ZAMG has been extremely helpful in field work logistics and data correspondence. The fieldwork was granted by INTERACT Transnational Access within the project ASEOM.

Finally I would like to thank my close friends and family for their unending/unconditional support during all my academic endeavours, especially during this difficult time of global pandemic and protest.

References

Adamovic, D. Doric, J., Vojinovic-Miloradov, M., Turk-Sekulic, M., Radonic, J., Krajinovic, S., Adamovic, S.: BTEX in the Exhaust Emissions of Motor Vehicles, *Global Conference on Global Warming*, (GCGW-2012) July 8 – 12, 2012.

Allen, S., Allen, D., Phoenix, V. R., Le Roux, G., Jiménez, P. D., Simonneau, A., Binet, S., Galop, D.: Atmospheric transport and deposition of microplastics in a remote mountain catchment, *Nature Geoscience*, vol 12, 339-334, https://doi.org/10.1038/s41561-019-0335-5, 2019.

Andreae, M. O., Browell, E. V., Garstang, M. et al.: Biomass-Burning Emissions and Associated Haze Layers Over Amazonia, *J. of Geophysical Research*, vol. 93, no. D2, pp 1509-1527, February 20, 1988.

Baimatova, N., Koziel, J. A., Kenessov, B.: Quantification of benzene, toluene, ethylbenzene and o-xylene in internal combustion engine exhaust with time-weighted average solid phase microextraction and gas chromatography mass spectrometry, *Analytica chimica acta,* 873, 38-50. DOI: 10.1016/j.aca.2015.02.062, 2015.

Bierbaum, V.M.,Golde, M.F. and Kaufman, F., J. Chem. Phys., 65, 2715, 1976.

Brahney, J., Hallerud, M., Heim, E., Hahnenberger, M., Sukumaran, S.: Plastic rain in protected areas of the United States, *Science*, 368, 1257–1260, 2020.

Brook, E.J., Ice Core Methods, Overview, in *Encyclopedia of Quaternary Science*, A.E. Scott, Editor. Elsevier: Oxford. 1145-1156, 2007.

Brunner, C., Szymczak, W., Höllriegl, V. et al.: Discrimination of cancerous and non-cancerous cell lines by headspace-analysis with PTR-MS, *Anal Bioanal Chem*, 397, 2315–2324,. https://doi.org/10.1007/s00216-010-3838-x, 2010.

Crutzen, P., Heidt, L., Krasnec, J. et al.: Biomass burning as a source of atmospheric gases CO, H_2, N_2O, NO, CH_3Cl and COS. *Nature* 282, pp 253–256, https://doi.org/10.1038/282253a0, 1979.

Dahl-Jensen, D.: Drilling for the oldest ice, *Nature Geoscience*, vol 11, pp 702–706, www.nature.com/naturegeoscience, October, 2018.

Déléris, I., Saint-Eve, A., Dakowski, F., Sémon, E., Le Quéré, J., Guillemin, H., Souchon, I.: The dynamics of aroma release during consumption of candies of different structures, and relationship with temporal perception, *Food Chemistry*, 127, 1615-1624, doi:10.1016/j.foodchem.2011.02.028, 2011.

Fiches, G., Déléris, I., Saint-Eve, A., Brunerie, P., Souchon, I.: Modifying PTR-MS operating conditions for quantitative headspace analysis of hydro-alcoholic beverages. 2. Brandy characterization and discrimination by PTR-MS, *International Journal of Mass Spectrometry*, 360, 15-23, http://dx.doi.org/10.1016/j.ijms.2013.11.010, 2014.

Fischer, H., Fundel, F., Ruth, U. et al.: Reconstruction of millennial changes in dust emission, transport and regional sea ice coverage using the deep EPICA ice cores from the Atlantic and Indian Ocean sector of Antarctica, *Earth and Planetary Science Letters*, 260 (2007) 340–354, 2007.

Geyer, R., Jambeck, J. R., Law, K. L.: Production, use, and fate of all plastics ever made, *Sci. Adv.*, 3, e1700782, 2017.

Hansel, A., Jordan, A., Holzinger, R., Prazeller, P., Vogel, W., Lindinger, W.: Proton transfer reaction mass spectrometry: on-line trace gas analysis at the ppb level, *International Journal of Mass Spectrometry and Ion Processes*, 149/150, 609-619, 1995.

Holzinger, R.: PTRwid: A New Widget-Tool for Processing PTR-TOF-MS Data, *Atmospheric Measurement Techniques*, 8, 3903–3922, www.atmos-meas-tech.net/8/3903/2015/, DOI:10.5194/amt-8-3903-2015, 2015.

Holzinger, R., Jordan, A., Hansel, A. & Lindinger, W.: Automobile Emissions of Acetonitrile: Assessment of its Contribution to the Global Source, *Journal of Atmospheric Chemistry*, 38: 187–193, 2001.

Holzinger, R., Warneke, C. Hansel, A., Jordan, A., Lindinger, W.: Biomass Burning as a Source of Formaldehyde, Acetaldehyde, Methanol, Acetone, Acetonitrile, and Hydrogen Cyanide, *Geophysical Research Letters*, vol. 26, no. 8, pgs 1161-1164, April15, 1999.

Holzinger, R.,Williams, J., Herrmann, F., Lelieveld, J., Donahue, N. M. & Röckmann, T.: Aerosol analysis using a Thermal-Desorption Proton-Transfer-Reaction Mass Spectrometer (TD-PTR-MS): a new approach to study processing of organic aerosols, *Atmos. Chem. Phys.*, 10, 2257–2267, 2010.

Jabali, O., Van Woensel, T., de Kok, A.G.: Analysis of Travel Times and CO_2 Emissions in Time-Dependent Vehicle Routing, *Productions and Operations Management*, vol. 21, no. 6, pp. 1060–1074, DOI: 10.1111/j.1937-5956.2012.01338.x, 2012.

Jordana, A., Haidacher, S., Hanel, G., Hartungena, E., Märka, L., Seehauser, H., Schottkowskya, R., Sulzer, P., Märka, T.D.: A high resolution and high sensitivity proton-transfer-reaction time-of-flight mass spectrometer (PTR-TOF-MS), *International Journal of Mass Spectrometry*, 286 (2009) 122–128, 2009.

Lambert, F., Delmonte, B., Petit, J. R., Bigler, M., Kaufmann, P. R., Hutterli, M. A., Stocker, T. F., Ruth, U., Steffensen, J. P., & Maggi, V.: Dust - climate couplings over the past 800,000 years from the EPICA Dome C ice core, *Nature*, vol 452, DOI:10.1038/nature06763, April 3, 2008.

Lias, S.G., Bartmess, J.E., Liebman, J.F., Holmes, J.L., Levin R.D. and Mallard, W.G.: J. Phys. Chem. Ref. Data, 17 (Suppl. 1), 1988.

Loader, N. J., McCarrol, D., Miles, D., Young, G., Davies, D. & Ramsey, C.: Tree ring dating using oxygen isotopes: a master chronology for central England, *J. Quaternary Sci*., vol. 34(6) 475–490, ISSN 0267-8179, DOI: 10.1002/jqs.3115, 2019.

Materić, D., Kasper-Giebl, A., Kau, D., Anten, M., Greilinger, M., Ludewig, E., van Sebille, E., Röckmann, T., & Holzinger, R.: Micro- and Nanoplastics in Alpine Snow: A New Method for Chemical Identification and (Semi)Quantification in the Nanogram Range, *Environmental Science and Technology*, 2020 54 (4), 2353-2359 DOI: 10.1021/acs.est.9b07540, 2020.

Materić, D., Ludewig, E., Xu, K., Röckmann, T., & Holzinger, R.: Brief Communication: Analysis of Organic Matter in Surface Snow by PTR-MS – Implications for Dry Deposition Dynamics in the Alps, *The Cryosphere*, 13, no. 1, 297–307. https://doi.org/10.5194/tc-13-297-2019, 2019.

Materić, D., Peacock, M., Kent, M., Cook, S., Gauci, V., Röckmann, T., & Holzinger, R.: Characterisation of the semi-volatile component of Dissolved Organic Matter by Thermal Desorption – Proton Transfer Reaction – Mass Spectrometry, *Sci. Reports*, 7: 15936, DOI: 10.1038/s41598-017-16256-x, 2017.

Moser, B., Bodrogo, F., Eibl, G., Lechner, M., Rieder, J., Lirk, P.: Mass spectrometric profile of exhaled breath—field study by PTR-MS, *Respiratory Physiology and Neurobiology*, 145, 295–300, 2005.

National Research Council, The Ongoing Challenge of Managing Carbon Monoxide Pollution in Fairbanks, Alaska: Interim Report. *Washington, DC: The National Academies Press*., pp 109-, https://doi.org/10.17226/10378, 2002.

Peacock, M., Materić, D., Kothawala, D. N., Holzinger, R., Futter, M. N.: Understanding Dissolved Organic Matter Reactivity and Composition in Lakes and Streams Using Proton-Transfer-Reaction Mass Spectrometry (PTR-MS), *Environmental Sci. and Tech. Letters*, 5, 739-744, DOI: 10.1021/acs.estlett.8b00529, 2018.

Tawfiq, M. F., Aroua, M. K., Sulaiman, N. M. N.: On-line CO, CO_2 emissions evaluation and (benzene, toluene, xylene) determination from experimental burn of tropical biomass, *J. of Environmental Sciences*, 33 239-244, http://dx.doi.org/10.1016/j.jes.2015.01.015, 2015.

Thompson, L. G., Mosley-Thompson, E., Davis, M. E., Lin, P.-N., Henderson, K. A., Cole-Dai, J., Bolzan, J. F., Liu, K.-b.: Late Glacial Stage and Holocene Tropical Ice Core Records from Huascaran, Peru, *Science*, DOI: 10.1126/science.269.5220.46, August, 1995.